the presence of 2 mM MgATP, 5 mM phosphocreatine, 5 U ml^{-1} creatine kinase and 2 mM succinate.

To carry out simultaneous measurements of $[Ca^{2+}]_c$ and $\Delta\Psi_m$, the permeabilized cells were supplemented with 0.5 μM fura2FF/FA and 800 nM JC1. Fluorescence was monitored in a multi-wavelength-excitation dual wavelength-emission fluorimeter (DeltaRAM, PTI) using 340- and 380-nm excitation and 535-nm emission for fura2FF whereas 490-nm excitation/535-nm emission and 570-nm excitation/595-nm emission were used for JC1. $\Delta\Psi_m$ is shown as the ratio of the fluorescence of J-aggregate (excitation 570 nm/emission 595 nm) and monomer (excitation 490 nm/emission 535 nm) forms of JC1. Calibration of fura2FF signal was carried out by adding $CaCl_2$ (2.5 mM) and subsequently EGTA/Tris (10 mM) at pH 8.5. Experiments were carried out at 35 °C and with simultaneous stirring.

Received 31 July; accepted 15 September 2003; doi:10.1038/nature02052.
Published online 8 October 2003.

1. Jones, J. M. *et al.* mnd2: a new mouse model of inherited motor neuron disease. *Genomics* **16,** 669–677 (1993).
2. Weber, J. S. *et al.* High-resolution genetic, physical, and transcript map of the mnd2 region of mouse chromosome 6. *Genomics* **54,** 107–115 (1998).
3. Rathke-Hartlieb, S. *et al.* Progressive loss of striatal neurons causes motor dysfunction in MND2 mutant mice and is not prevented by Bcl-2. *Exp. Neurol.* **175,** 87–97 (2002).
4. Jang, W. *et al.* Comparative sequence of human and mouse BAC clones from the mnd2 region of chromosome 2p13. *Genome Res.* **9,** 53–61 (1999).
5. Jang, W., Weber, J. S., Bashir, R., Bushby, K. & Meisler, M. H. Aup1, a novel gene on mouse chromosome 6 and human chromosome 2p13. *Genomics* **36,** 366–368 (1996).
6. Jang, W., Weber, J. S., Harkins, E. B. & Meisler, M. H. Localization of the rhotekin gene RTKN on the physical maps of mouse chromosome 6 and human chromosome 2p13 and exclusion as a candidate for mnd2 and LGMD2B. *Genomics* **40,** 506–507 (1997).
7. Jang, W., Weber, J. S., Tokito, M. K., Holzbaur, E. L. & Meisler, M. H. Mouse p150Glued (dynactin 1) cDNA sequence and evaluation as a candidate for the neuromuscular disease mutation mnd2. *Biochem. Biophys. Res. Commun.* **231,** 344–347 (1997).
8. Ji, W. *et al.* DQX1, an RNA-dependent ATPase homolog with a novel DEAQ box: expression pattern and genomic sequence comparison of the human and mouse genes. *Mamm. Genome* **12,** 456–461 (2001).
9. Li, W. *et al.* Structural insights into the pro-apoptotic function of mitochondrial serine protease HtrA2/Omi. *Nature Struct. Biol.* **9,** 436–441 (2002).
10. Hegde, R. *et al.* Identification of Omi/HtrA2 as a mitochondrial apoptotic serine protease that disrupts inhibitor of apoptosis protein-caspase interaction. *J. Biol. Chem.* **277,** 432–438 (2002).
11. Suzuki, Y. *et al.* A serine protease, HtrA2, is released from the mitochondria and interacts with XIAP, inducing cell death. *Mol. Cell* **8,** 613–621 (2001).
12. Verhagen, A. M. *et al.* HtrA2 promotes cell death through its serine protease activity and its ability to antagonize inhibitor of apoptosis proteins. *J. Biol. Chem.* **277,** 445–454 (2002).
13. Martins, L. M. *et al.* The serine protease Omi/HtrA2 regulates apoptosis by binding XIAP through a reaper-like motif. *J. Biol. Chem.* **277,** 439–444 (2002).
14. van Loo, G. *et al.* The serine protease Omi/HtrA2 is released from mitochondria during apoptosis. Omi interacts with caspase-inhibitor XIAP and induces enhanced caspase activity. *Cell Death Differ.* **9,** 20–26 (2002).
15. Clausen, T., Southan, C. & Ehrmann, M. The HtrA family of proteases: implications for protein composition and cell fate. *Mol. Cell* **10,** 443–455 (2002).
16. Maurizi, M. R. Love it or cleave it: tough choices in protein quality control. *Nature Struct. Biol.* **9,** 410–412 (2002).
17. Srinivasula, S. M. *et al.* Inhibitor of apoptosis proteins are substrates for the mitochondrial serine protease Omi/HtrA2. *J. Biol. Chem.* **278,** 31469–31472 (2003).
18. Yang, Q. H., Church-Hajduk, R., Ren, J., Newton, M. L. & Du, C. Omi/HtrA2 catalytic cleavage of inhibitor of apoptosis (IAP) irreversibly inactivates IAPs and facilitates caspase activity in apoptosis. *Genes Dev.* **17,** 1487–1496 (2003).
19. Brustovetsky, N. *et al.* Increased susceptibility of striatal mitochondria to calcium-induced permeability transition. *J. Neurosci.* **23,** 4858–4867 (2003).
20. Szalai, G., Krishnamurthy, R. & Hajnoczky, G. Apoptosis driven by IP(3)-linked mitochondrial calcium signals. *EMBO J.* **18,** 6349–6361 (1999).
21. Reed, J. C. Cytochrome c: can't live with it—can't live without it. *Cell* **91,** 559–562 (1997).
22. Joza, N. *et al.* Essential role of the mitochondrial apoptosis-inducing factor in programmed cell death. *Nature* **410,** 549–554 (2001).
23. Klein, J. A. *et al.* The harlequin mouse mutation downregulates apoptosis-inducing factor. *Nature* **419,** 367–374 (2002).
24. Walsh, N. P., Alba, B. M., Bose, B., Gross, C. A. & Sauer, R. T. OMP peptide signals initiate the envelope-stress response by activating DegS protease via relief of inhibition mediated by its PDZ domain. *Cell* **113,** 61–71 (2003).
25. Leist, M., Single, B., Castoldi, A. F., Kuhnle, S. & Nicotera, P. Intracellular adenosine triphosphate (ATP) concentration: a switch in the decision between apoptosis and necrosis. *J. Exp. Med.* **185,** 1481–1486 (1997).
26. Susin, S. A. *et al.* Molecular characterization of mitochondrial apoptosis-inducing factor. *Nature* **397,** 441–446 (1999).
27. Danial, N. N. *et al.* BAD and glucokinase reside in a mitochondrial complex that integrates glycolysis and apoptosis. *Nature* **424,** 952–956 (2003).
28. Casari, G. *et al.* Spastic paraplegia and OXPHOS impairment caused by mutations in paraplegin, a nuclear-encoded mitochondrial metalloprotease. *Cell* **93,** 973–983 (1998).
29. Van Dyck, L. & Langer, T. ATP-dependent proteases controlling mitochondrial function in the yeast *Saccharomyces cerevisiae*. *Cell. Mol. Life Sci.* **56,** 825–842 (1999).

Acknowledgements This work was supported by grants from the National Institutes of Health and the Muscular Dystrophy Association. S.M.S. is a Kimmel scholar. W.J. acknowledges support from the Hearing and Chemical Senses Training Program of the University of Michigan. We thank J. Zhang for help in preparation of MEFs and A. Zervos for the mouse Omi cDNA. We also thank M. Farrer and T. Gasser for the PARK3 DNA samples.

Competing interests statement The authors declare that they have no competing financial interests.

Authors' contributions J.M.J., P.D., S.M.S. and W.J. share equal first authorship and E.S.A. and M.H.M. share equal senior authorship.

Correspondence and requests for materials should be addressed to E.S.A. (E_Alnemri@lac.jci.tju.edu) or M.H.M. (meislerm@umich.edu).

Functional cloning of TUG as a regulator of GLUT4 glucose transporter trafficking

Jonathan S. Bogan[1,2,3]*, Natalie Hendon[1,2], Adrienne E. McKee[1]*, Tsu-Shuen Tsao[1] & Harvey F. Lodish[1,4]

[1]*Whitehead Institute for Biomedical Research, Cambridge, Massachusetts 02142, USA*
[2]*Diabetes Unit, Department of Medicine, Massachusetts General Hospital, Boston, Massachusetts 02129, USA*
[3]*Department of Medicine, Harvard Medical School, Boston, Massachusetts 02114, USA*
[4]*Department of Biology, Massachusetts Institute of Technology, Cambridge, Massachusetts 02142, USA*

* Present addresses: Section of Endocrinology and Metabolism, Department of Internal Medicine, Yale University School of Medicine, 333 Cedar Street, Box 208020, New Haven, Connecticut 06520-8020, USA (J.S.B.); Program in Biological and Biomedical Sciences, Harvard Medical School, 220 Longwood Ave, Boston, Massachusetts 02115, USA (A.E.M.)

Insulin stimulates glucose uptake in fat and muscle by mobilizing the GLUT4 glucose transporter. GLUT4 is sequestered intracellularly in the absence of insulin, and is redistributed to the plasma membrane within minutes of insulin stimulation[1,2]. But the trafficking mechanisms that control GLUT4 sequestration have remained elusive. Here we describe a functional screen to identify proteins that modulate GLUT4 distribution, and identify TUG as a putative tether, containing a UBX domain, for GLUT4. In truncated form, TUG acts in a dominant-negative manner to inhibit insulin-stimulated GLUT4 redistribution in Chinese hamster ovary cells and 3T3-L1 adipocytes. Full-length TUG forms a complex specifically with GLUT4; in 3T3-L1 adipocytes, this complex is present in unstimulated cells and is largely disassembled by insulin. Endogenous TUG is localized with the insulin-mobilizable pool of GLUT4 in unstimulated 3T3-L1 adipocytes, and is not mobilized to the plasma membrane by insulin. Distinct regions of TUG are required to bind GLUT4 and to retain GLUT4 intracellularly in transfected, non-adipose cells. Our data suggest that TUG traps endocytosed GLUT4 and tethers it intracellularly, and that insulin mobilizes this pool of retained GLUT4 by releasing this tether.

The proportion of GLUT4 at the surface of individual living cells was assayed by using flow cytometry to measure fluorescence intensities corresponding to cell surface and total GLUT4. For this, we used a previously described GLUT4 reporter protein containing epitope tags in its first extracellular domain and green fluorescent protein (GFP) at the carboxy terminus[3]. To identify proteins that alter GLUT4 distribution, we constructed a 3T3-L1 adipocyte complementary DNA library in a retroviral vector. We used the pMX-IRES-CD2 vector because it produces a bicistronic

message encoding both the cloned cDNA and the extracellular portion of CD2 antigen, which makes it easier to identify infected cells[4]. We infected a clonal Chinese hamster ovary (CHO) cell line expressing the GLUT4 reporter and the murine ecotropic retrovirus receptor, such that 34% of $\sim 5 \times 10^7$ target cells became CD2 positive. At this viral titre, statistics suggest that almost all of the infected cells received only one retrovirus from the library. Expression of each cDNA is stable because the retrovirus integrates into the genome. We enriched particular cDNAs within the library that, when overexpressed, alter trafficking of the GLUT4 reporter.

Our previous data support the notion that, in CHO cells cultured with abundant amino acids, insulin mobilizes GLUT4 to the plasma membrane from endosomes and a poorly defined, highly insulin-responsive compartment that may be similar to that found in 3T3-L1 adipocytes[3]. We considered that 5 min after insulin addition, but not necessarily after more prolonged stimulation, most of the increased GLUT4 at the cell surface will come from the highly insulin-responsive compartment. Thus, to bias our cloning strategy towards proteins involved in trafficking through this compartment, we cultured CHO cells containing the cDNA library in an abundance of amino acids and stimulated cells with insulin for 5 min only. We then chilled the cells and prepared them for flow cytometry. To identify cells that had either enhanced or diminished translocation of GLUT4, we used an iterative enrichment process in which we first sorted the ~0.2% of cells with the highest or lowest ratio of fluorescence intensities. We expanded the sorted cells in culture, then restimulated the expanded cells with insulin and subjected them to further enrichment by flow sorting. Figure 1a illustrates this approach to enriching cells with diminished translocation of GLUT4. For the third flow cytometry step, our sorting criteria were less stringent, and we cloned individual cells in 96-well plates if they fell within the ~1% of the population with the highest or lowest ratio of fluorescence intensities. We predicted that after three iterations of sorting and expansion, the overall enrichment would be $>10^7$-fold, which is sufficient to isolate individual cDNAs from the library. Of the 150 clonal cell lines isolated, 77% were CD2 positive. Most (142/150) of these cell lines had increased GLUT4 at the cell surface, because cloning efficiency was poor for cells with

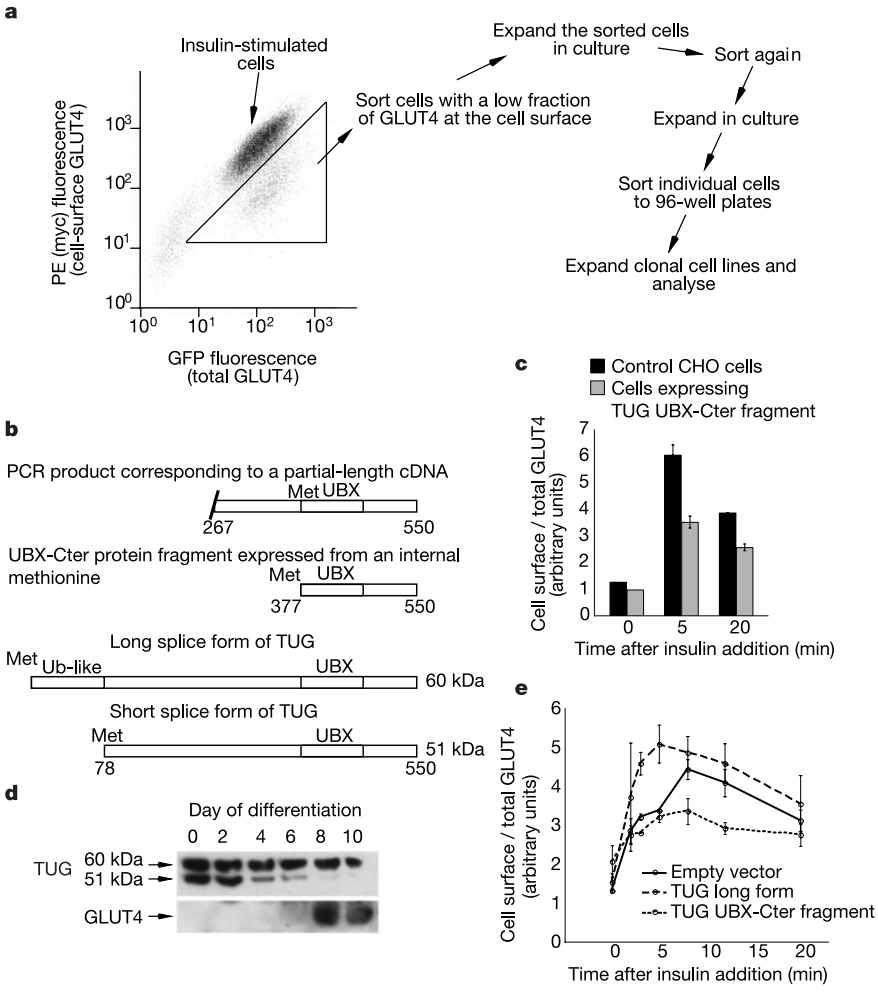

Figure 1 Expression cloning of TUG. **a**, Enrichment process in cells with a low ratio of surface to total GLUT4. See main text and Methods for more details. Note that the upper diagonal edge of the population (high surface:total GLUT4) is sharper than the lower diagonal edge of the population (low surface: total GLUT4) owing to fewer dead or poorly stained cells, permitting a more stringent sorting gate. **b**, PCR of proviral insertions from genomic DNA of two clones yielded identical 1.2-kb products. This sequence contained a partial-length open reading frame, which spans TUG residues 267–550 and contains a UBX domain. Translation beginning at the first methionine is predicted to produce a protein fragment known as UBX-Cter (residues 377–550). The full-length TUG protein is present in two splice forms. The longer of these forms contains a region at its N terminus with similarity to ubiquitin. **c**, Expression of TUG UBX-Cter inhibits the ability of insulin to redistribute GLUT4 in CHO cells. **d**, The short form of TUG is downregulated during adipose differentiation, whereas the long form persists and is expressed together with GLUT4 in differentiated adipocytes. **e**, Opposite effects of expression of the long form of TUG and of TUG UBX-Cter on GLUT4 trafficking in 3T3-L1 adipocytes. Measurements were made in triplicate, and error bars indicate standard deviation.

decreased GLUT4 translocation. We prepared genomic DNA from selected CD2-positive cell lines with consistently altered GLUT4 trafficking, and used polymerase chain reaction (PCR) with primers from sequences in the retroviral vector to identify the inserted cDNAs.

Two out of the eight clones isolated in the screen for cells with a low fraction of GLUT4 at the cell surface had a particularly robust phenotype, and PCR of genomic DNA from these clones yielded identical 1.2-kilobase (kb) products. Sequencing identified an 852-nucleotide reading frame encoding the C terminus of a novel protein, which we call TUG (tether, containing a UBX domain, for GLUT4) (Fig. 1b). We reasoned that the cloned sequence would produce a protein fragment initiated at the first encoded methionine; this fragment would correspond to the C terminus of full-length TUG. Searches of the murine expressed sequence tag (EST) database identified two splice forms of TUG. The longer of these contains a sequence at the amino terminus with similarity to ubiquitin, and is predicted to be 550 residues long. The probable start codon in the short form is equivalent to methionine 78 of the long form. By this numbering, the C-terminal fragment might start at methionine 377, which is normally an internal residue. Database searches identified a 79-residue UBX domain in the predicted TUG protein. Other proteins containing this domain include p47, an adaptor protein that recruits the NSF (*N*-ethylmaleimide-sensitive factor)-like p97 ATPase in the fusion of Golgi and transitional endoplasmic reticulum (ER) membranes with FAF1 (Fas-associated factor 1), a protein that binds to Fas and regulates apoptosis[5,6]. The structures of the UBX domains in p47 and FAF1 indicate that they form a ubiquitin-like, β-grasp structure[7,8].

The C-terminal TUG fragment we predicted to be produced by our initial clone contains this UBX domain (Fig. 1b), and we therefore refer to this fragment as TUG UBX-Cter. We further considered that production of UBX-Cter might alter the insulin-stimulated translocation of GLUT4. Consistent with this hypothesis, expression of UBX-Cter substantially inhibits the ability of insulin to redistribute GLUT4 in CHO cells (Fig. 1c). These results show that our cloning strategy was successful and, together with the data presented below, indicate that this fragment acts in a dominant-negative manner to block the insulin signal required to redistribute GLUT4.

During our study, the probable human homologue of TUG was identified as part of a fusion protein found in alveolar soft-part sarcomas[9]. This protein, termed ASPL, is 76% identical to murine TUG and also undergoes alternative splicing. Both TUG and ASPL are widely expressed[9] (Supplementary Fig. 1). Antisera raised against the C terminus of TUG/ASPL were specific when used for immunoblotting or immunofluorescence microscopy (Supplementary Fig. 2). In 3T3-L1 cells, immunoblotting shows that the short form of TUG is downregulated during adipose differentiation, whereas the long form persists and is expressed together with GLUT4 in differentiated adipocytes (Fig. 1d). We conclude, from this and the data below, that it is the long form of TUG that controls GLUT4 distribution in 3T3-L1 adipocytes.

To determine whether the C-terminal fragment of TUG inhibits insulin-stimulated GLUT4 translocation in 3T3-L1 adipocytes as well as in CHO cells, we expressed UBX-Cter by retrovirally infecting cells expressing the GLUT4 reporter. As shown in Fig. 1e, expression of this truncated protein substantially inhibits the degree to which insulin increases GLUT4 at the plasma membrane. Some of this effect is due to increased GLUT4 at the plasma membrane in the absence of insulin; this increase was not observed in CHO cells, which are a poorer adipocyte model. Overexpression of the full-length TUG long form in 3T3-L1 adipocytes increases the rapidity and initial magnitude of GLUT4 movement to the surface after insulin stimulation. Thus, truncated and full-length forms of TUG have opposite effects on insulin-stimulated movement of GLUT4 when they are expressed exogenously in 3T3-L1 adipocytes. The full-length TUG protein enhances the normal action of insulin,

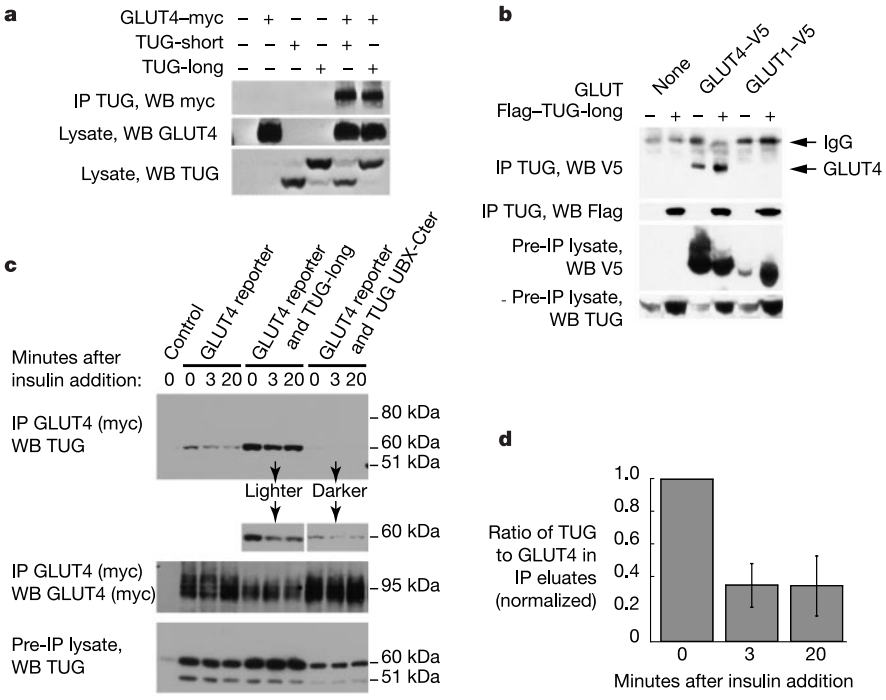

Figure 2 Interaction of TUG with GLUT4. **a**, Immunoprecipitation of either the long or short form of TUG co-purifies myc-tagged GLUT4 in transfected 293T cells. **b**, The interaction of TUG with GLUT4 is specific, because GLUT1 containing an identical epitope tag is not co-immunoprecipitated. **c**, Interaction of endogenous TUG with GLUT4 in 3T3-L1 adipocytes. Insulin decreases the amount of TUG immunoprecipated with GLUT4. Expression of the TUG long form increases the amount of TUG that is co-purified with GLUT4, and expression of TUG UBX-Cter decreases this amount. **d**, Insulin decreases the amount of TUG complexed with GLUT4. Measurements were in quadruplicate, and error bars indicate standard deviation.

whereas the UBX-Cter fragment acts in a dominant-negative fashion to inhibit the insulin-stimulated movement of GLUT4. As detailed below, we believe that overexpression of TUG increases the fraction of GLUT4 that accumulates in an intracellular, insulin-mobilizable pool in unstimulated cells.

To determine whether the effects of truncated and full-length TUG overexpression in 3T3-L1 adipocytes are specific to GLUT4, we immunoblotted plasma-membrane fractions to detect endogenous GLUT4, GLUT1 and the transferrin receptor (TfnR). We treated cells briefly with insulin to detect the peak of the translocation response. As shown in Supplementary Fig. 3, insulin markedly increases GLUT4 in plasma membranes of control cells, and this effect is enhanced by overexpression of full-length TUG and is blocked by expression of the UBX-Cter fragment. These data are consistent with the results shown in Fig. 1e. Insulin slightly increases the amounts of GLUT1 and TfnR in plasma membranes of control cells. Exogenous expression of full-length TUG or UBX-Cter fragment has little effect on the insulin-stimulated increase in plasma-membrane GLUT1 and TfnR. We immunoblotted the insulin receptor β-subunit as a negative control; as expected, insulin did not alter the amount of β-subunit present in the plasma membranes.

We also examined whether TUG influences the ability of insulin to regulate 2-deoxyglucose uptake in 3T3-L1 adipocytes. We found that insulin stimulates glucose uptake by 3.6-fold in control cells (95% confidence interval, 1.6-fold to 8.3-fold), by 3.5-fold in cells stably expressing the long form of TUG (1.9-fold to 6.3-fold) and by 0.73-fold in cells stably expressing the TUG UBX-Cter fragment (0.54-fold to 1.0-fold). Total amounts of GLUT4 and GLUT1 were similar in all samples as judged by immunoblotting, and exogenous expression of TUG or of the UBX-Cter fragment had no effect on 3T3-L1 differentiation (data not shown). Thus, TUG UBX-Cter blocks the ability of insulin to stimulate glucose uptake, and this effect cannot be attributed to altered glucose transporter levels. Taken together, the data indicate that TUG specifically links insulin action with GLUT4 movement, and its action modulates deoxyglucose uptake in 3T3-L1 adipocytes.

To gain insight into how a UBX-domain-containing protein controls GLUT4 trafficking, we reviewed the functions of other proteins containing this domain. One such protein, FAF1, binds to wild-type Fas but not to the allele of Fas found in *lpr*^{cg} mice, which has a single point mutation in its cytoplasmic domain[6]. Comparison of the sequences of GLUT4 and Fas revealed a small region of local similarity (236-EAKKFARENNI-246 in Fas and 263-EKRKLERERPL-273 in GLUT4) within the large cytoplasmic loop between the sixth and seventh transmembrane domains of GLUT4. More significantly, the I246N mutation in the Fas *lpr*^{cg} allele falls within this motif and corresponds to a similar residue (L273) in GLUT4. In

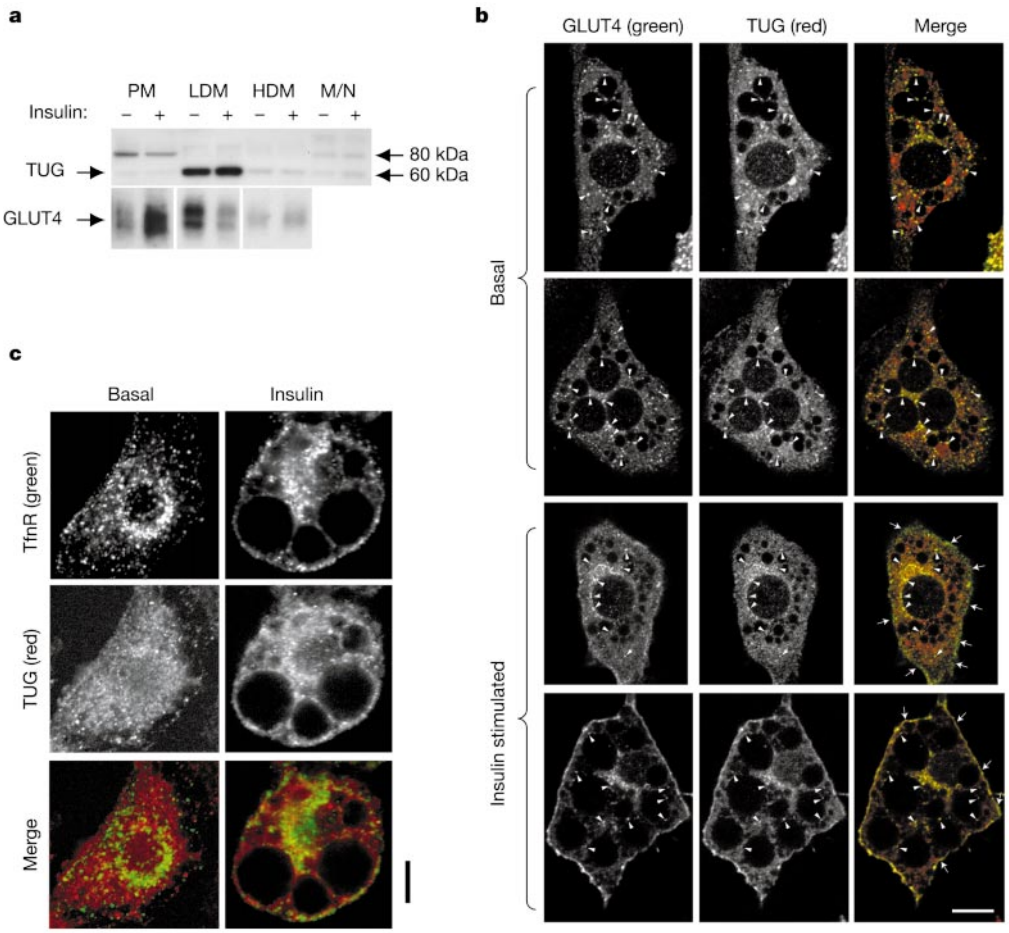

Figure 3 Subcellular localization of TUG. **a**, Basal and stimulated 3T3-L1 adipocytes were subjected to differential centrifugation to isolate fractions enriched in plasma membranes (PM), low-density microsomes (LDM), high-density microsomes (HDM) and mitochondria and nuclei (M/N). Equal amounts of protein from each fraction were immunoblotted with anti-TUG and anti-GLUT4 antibodies. **b**, Basal and stimulated 3T3-L1 adipocytes expressing the GLUT4 reporter were stained to detect anti-GLUT4 (green) and anti-TUG (red) antibodies. Images were acquired by confocal microscopy. Arrowheads indicate colocalization. Arrows show regions of plasma-membrane staining for GLUT4 but not TUG. Bar, 10 μM. **c**, Basal and stimulated 3T3-L1 adipocytes were stained using anti-TfnR (green) and anti-TUG (red) antibodies. Images were acquired by confocal microscopy. Bar, 10 μM.

addition, Ubc9, a conjugating enzyme for the ubiquitin-like protein Sumo, binds to Fas and GLUT4 (refs 10–12). Daxx is another protein recently reported to interact with GLUT4 as well as with Fas[13]. Therefore, we proposed that similar complexes involving Ubc9, Daxx and a UBX-containing protein form with Fas and GLUT4. To test the prediction that GLUT4 and TUG interact, we performed co-immunoprecipitation experiments using transiently transfected 293T cells. Immunoprecipitation of either the long or the short form of TUG co-purifies myc-tagged GLUT4 (Fig. 2a). This interaction is specific for GLUT4, because GLUT1 is not co-purified in similar co-transfection experiments (Fig. 2b); some GLUT4 is even immunoprecipitated with endogenous TUG. These data are consistent with those in Supplementary Fig. 3, which implicate TUG in GLUT4 but not GLUT1 trafficking. Thus, TUG complexes interact specifically with GLUT4 in transfected cells, and the N-terminal ubiquitin-like domain of TUG is not required for this interaction.

To determine whether endogenous TUG interacts with GLUT4 in 3T3-L1 adipocytes, we used cells expressing the GLUT4 reporter; this tagged protein is expressed at approximately fivefold higher levels than endogenous GLUT4 in mature 3T3-L1 adipocytes (data not shown). We stimulated cells with insulin for various times, then prepared lysates and immunoprecipitated the reporter using an anti-myc affinity matrix. TUG was present in the eluted material (Fig. 2c), which further demonstrates that insulin decreases the amount of TUG that immunoprecipitates with GLUT4. Densitometric analysis indicates that insulin reduces by two-thirds the amount of TUG that is complexed with GLUT4 (Fig. 2d). In cells overexpressing the long form of TUG, which accelerates the mobilization of GLUT4 after insulin addition, more TUG immunoprecipitates with GLUT4. Conversely, in cells expressing TUG UBX-Cter, less TUG is co-immunoprecipitated. In all cases, insulin decreases the association between TUG and GLUT4. Thus, TUG and GLUT4 form complexes in 3T3-L1 adipocytes, and insulin stimulates disassembly of most of these complexes.

To assess the subcellular distribution of endogenous TUG, we fractionated 3T3-L1 adipocytes using a standard differential centrifugation protocol. TUG is present in approximately equal amounts in the cytosol and in membranes (data not shown); membrane-associated TUG is present predominantly in the low-density microsomal fraction (Fig. 3a); the same fraction contains the highly insulin-responsive pool of GLUT4. In contrast to GLUT4, we observed no marked movement of TUG after insulin stimulation. In addition to the expected 60-kDa band corresponding to the long form of TUG, we observe an 80-kDa band in the plasma-membrane fraction. This 80-kDa band may be a cross-reacting protein. Another possibility is that it is a form of TUG that is modified by covalent addition of a ubiquitin-like protein, because our antisera seem to be specific (Supplementary Fig. 2a) and the Sumo-conjugating protein Ubc9 also binds to GLUT4 (ref. 10). The 80-kDa protein is not present in material immunoprecipitated with GLUT4, and therefore does not form a stable complex with GLUT4 (Fig. 2c).

To test the colocalization of TUG and GLUT4, we performed confocal immunofluorescence microscopy of 3T3-L1 adipocytes expressing the GLUT4 reporter. As shown in Fig. 3b, TUG has a homogeneous distribution, corresponding to cytosolic protein, and an overlying punctate and perinuclear distribution, corresponding to membrane-associated TUG. In unstimulated cells, most TUG punctae localize with GLUT4 (arrowheads), which is present in its characteristic vesicular and perinuclear pattern. After insulin addition, GLUT4 is clearly visible at the plasma membrane, and there seem to be fewer intracellular punctae where GLUT4 and TUG overlap. TUG is also present at or near the plasma membrane,

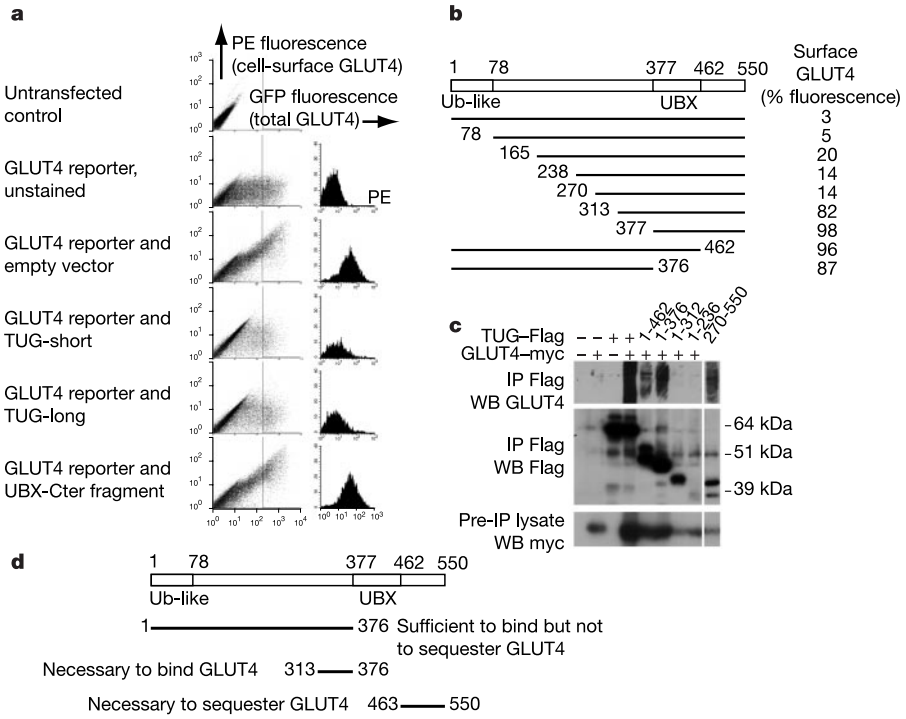

Figure 4 Mapping of TUG domains in non-adipose cells. **a**, Expression of either the long or the short form of TUG reduces the appearance of GLUT4 at the surface, as detected by flow cytometry. The histograms to the right indicate the distribution of phycoethrin (PE), which corresponds to cell-surface GLUT4. **b**, Deletion of the N terminus to residue 165 slightly reduces retention of GLUT4, as assessed by PE fluorescence. Deletions beyond residue 270 prevent TUG from sequestering GLUT4. Deletion of the C terminus also prevents sequestration. **c**, Truncation of C-terminal residues 377–550 and 463–550 does not impair immunoprecipitation of GLUT4. N-terminal truncations of residues 1–269 do not impair immunoprecipitation either. **d**, A summary of the regions of TUG that are (1) sufficient to bind GLUT4 in immunoprecipitation experiments, (2) necessary for this interaction, and (3) necessary to sequester GLUT4 in transfected cells but not required to form a complex with GLUT4.

although to a lesser extent than GLUT4 in insulin-stimulated cells; there are clear regions at the cell surface that stain for GLUT4 but not TUG (arrows). The TUG observed at the plasma membrane may correspond to the 80-kDa band seen by subcellular fractionation (Fig. 3a). To determine whether the punctae labelled with the TUG antibody correspond to endosomes, we acquired confocal images of 3T3-L1 adipocytes stained to detect endogenous TUG and TfnR. These proteins have distinct and non-overlapping distributions (Fig. 3c). Thus, TUG and GLUT4 colocalize on intracellular, insulin-responsive membranes that are distinct from TfnR-containing endosomes, and TUG may also be present at or near the plasma membrane in a covalently modified form.

Our data suggest that TUG is an essential part of the mechanism by which GLUT4 is sequestered in unstimulated cells. In this model, intracellular GLUT4 is trapped by a complex comprising TUG and probably other proteins, which stably associates with GLUT4 and retains it in intracellular, non-endosomal membranes by binding to an unknown anchoring protein. To test directly whether TUG sequesters GLUT4 in non-adipose cells, we performed flow cytometry of 293T cells transiently transfected with the GLUT4 reporter with or without TUG. Co-expression of either form of TUG greatly reduces the appearance of GLUT4 at the surface (Fig. 4a). In these co-transfections, the fluorescent signal corresponding to cell-surface GLUT4 is only 3–5% of that in control cells not transfected with TUG. These data are consistent with those in Fig. 1e and Supplementary Fig. 3, in which overexpression of the full-length form of TUG apparently increased the size of the rapidly insulin-mobilizable intracellular pool of GLUT4 in unstimulated 3T3-L1 adipocytes. Co-transfection of the truncated TUG UBX-Cter fragment does not cause intracellular retention of GLUT4 in 293T cells, consistent with the idea that this fragment blocks formation of a complex required for GLUT4 retention.

To map the regions of TUG required to sequester GLUT4, we co-transfected 293T cells with various truncations of TUG and the GLUT4 reporter, and, similar to Fig. 4a, assayed cell-surface GLUT4 by flow cytometry. Deletion of the N terminus to residue 165 modestly decreases the ability of TUG to retain GLUT4 intracellularly (Fig. 4b). Further deletions of the N terminus, from residue 270 to 313 or beyond, prevent TUG from sequestering GLUT4, as does deletion of residues to 462 or beyond from the C terminus of TUG. In complementary experiments, we sought to determine by co-immunoprecipitation which regions of TUG complex with GLUT4. Truncation of the C terminus of TUG (residues 377–550 or 463–550) does not impair its ability to co-immunoprecipitate GLUT4 (Fig. 4c). Likewise, an N-terminal truncation (of residues 1–269) still co-immunoprecipitates GLUT4. Thus, residues 1–376 of TUG are sufficient to complex with GLUT4, but not sufficient to retain it in non-adipose cells. Within this region, residues 313–376 are necessary to form the complex: truncation of these residues abrogates GLUT4 co-immunoprecipitation. Finally, the C terminus of TUG (residues 463–550) is required to retain GLUT4 intracellularly within non-adipose cells but not for the interaction of TUG with GLUT4. This region may bind an intracellular anchor to retain the TUG–GLUT4 complex within cells.

Insulin regulates glucose homeostasis on a minute-to-minute basis by controlling glucose use by muscle and fat[1,2,14]. Trafficking of GLUT4 is crucial for this regulation, and insulin probably acts at several steps in the GLUT4 recycling pathway to control its subcellular distribution. After endocytosis from the plasma membrane, GLUT4 is sorted away from endosomes to a highly insulin-responsive compartment, where it is selectively retained. Some data suggest that endocytosed GLUT4 moves through the trans-Golgi network (TGN); if so, this step might precede its arrival in the insulin-responsive compartment, or the insulin-responsive pool might participate in an intracellular cycle through the TGN[1,15]. Our data are compatible with these models, and TUG could retain GLUT4 in post-TGN membranes or constrain a dynamic intracellular cycle. Most biochemical and kinetic data are consistent with a three-compartment model in which GLUT4 is present predominantly in the plasma membrane, endosomes/TGN and insulin-responsive membranes[2,3]. In this model, TUG binds endocytosed GLUT4 through its N-terminal and central domains and retains it in post-endocytic, insulin-responsive membranes through its C terminus; presumably, the C terminus binds an unidentified intracellular anchor. Insulin mobilizes this pool of retained GLUT4 by disrupting the interaction between TUG and GLUT4. Thus, the data suggest that in adipocytes the long form of TUG tethers a highly insulin-responsive pool of GLUT4.

The effects of TUG overexpression on the transient characteristics of insulin-stimulated GLUT4 translocation are consistent with the above interpretation. Our previous data show that insulin-stimulated movement of GLUT4 is characterized by a brief overshoot of the steady-state distribution[3]. This response is cell-type-specific, and is consistent with a three-compartment model for GLUT4 trafficking. GLUT4 mobilized from the insulin-responsive, non-endosomal compartment accounts for the overshoot. It is significant that overexpression of TUG increases the rapidity and initial magnitude of GLUT4 translocation, which is exactly what would be predicted if the size of the insulin-mobilized pool were increased. Therefore, the data in Fig. 1e and Supplementary Fig. 3 provide an essential functional corroboration of the binding and colocalization data in Figs 2 and 3. Moreover, confocal microscopy indicates that most intracellular, non-endosomal GLUT4 localizes with TUG, consistent with the idea that this represents a relatively stable pool in the absence of insulin.

We do not yet know the insulin signaling pathway(s) that causes dissociation of TUG and GLUT4. This dissociation occurs soon after insulin addition and precedes significant movement of GLUT4 (ref. 3). Insulin signals through at least two distinct mechanisms to redistribute GLUT4; these involve phosphatidylinositol-3-kinase activation, which signals to Akt and perhaps to other proteins, as well as a CAP–Cbl–TC10 pathway leading to the mammalian exocyst complex and probably to other effectors[16,17]. These pathways may act on different steps in the GLUT4 recycling pathway; for example, one signal may move GLUT4 out of an intracellular, insulin-responsive compartment, and another may stimulate fusion of vesicles containing GLUT4 at the plasma membrane[2]. We find that the TUG UBX-Cter fragment disrupts the interaction of GLUT4 and native TUG; unstimulated cells expressing this fragment have slightly increased GLUT4 at the plasma membrane, and insulin-induced GLUT4 translocation is markedly inhibited. Expression of the UBX-Cter fragment probably prevents GLUT4 from being retained in an insulin-responsive pool but is not sufficient to bypass other regulated steps in the recycling pathway. GLUT4 might pass through the insulin-regulated compartment to be loaded onto molecular motors containing the unconventional myosin Myo1c, which could maintain a rapid exocytosis rate (compared with endosome recycling) in the presence of insulin[18].

The observation that some TUG is at or near the plasma membrane of cells treated with insulin raises the possibility that TUG positions GLUT4 near the plasma membrane after insulin stimulation. It is interesting that the TUG antisera detect an 80-kDa band in the plasma membrane fraction. Given the likely presence of Ubc9 in the complex, it may be that this band represents TUG that has been modified with a ubiquitin-like protein. Sumo and other ubiquitin-like modifications regulate the intracellular targeting of proteins[19]. Insulin might stimulate the covalent modification of TUG; this may be transient but nonetheless sufficient to target it, together with GLUT4, to the plasma membrane.

Our data show that both forms of TUG can bind and sequester GLUT4 in transfected cells, yet only the long form is expressed in mature 3T3-L1 adipocytes. One possibility is that the relative amounts of long and short TUG forms control the ability of insulin to mobilize tethered GLUT4. For example, it may be that only

GLUT4 that is retained by the long form of TUG is mobilized by insulin, and that the short form of TUG tethers GLUT4 in a non-insulin-responsive pool. If so, the ability of insulin to control glucose uptake might be controlled at the level of TUG transcription. We do not know whether the long or short splice forms of TUG are targets of insulin action in muscle, nor whether TUG has any role in contraction-mediated GLUT4 translocation. Nonetheless, TUG may have an important role in controlling organism-level glucose homeostasis, and variations in this protein may predispose humans to insulin resistance characteristic of type 2 diabetes mellitus. □

Methods

Library construction, retroviral infection and cell culture

A cDNA library was constructed from 3T3-L1 adipocyte poly-A + RNA using a combination of oligo-dT and random hexamer priming for first-strand synthesis (Superscript, Life Technologies). cDNAs were cloned non-directionally in the *Bst*XI sites of the pMX-IRES-CD2 vector[4]. The total complexity of the library was calculated at $>2.4 \times 10^6$ independent clones, with >90% of clones having inserts. The retrovirus was produced by transient transfection of 293-based packaging lines as described previously[3], except that pCL-Eco was co-transfected to increase viral titres[20]. Virus was used to infect CHO cells expressing the GLUT4 reporter as described previously[3]. For experiments in which cloned forms of the TUG cDNA were expressed from a retrovirus, the pBICD2 vector was used. pBICD2 was identical to pMX-IRES-CD2 except that point mutations were introduced to eliminate two potential translation start sites 5′ of the cloning site (J.S.B., A.E.M., X. Liu and H.F.L., unpublished data). Cell culture and flow cytometry, including measurement of GLUT4 trafficking, were performed as described previously[3].

Cloning and database searches

Genomic DNA was prepared from clonal cell lines using a Qiagen kit, and proviral insertions were amplified by PCR primed from retroviral vector sequences. The full-length TUG short form cDNA was cloned from an arrayed liver cDNA library (Origene). Additional sequence for the full-length TUG long-form cDNA was identified using overlapping ESTs, and this sequence was PCR-amplified from skeletal muscle cDNA (Invitrogen). Truncated cDNAs were cloned using pcDNA3.1-TOPO (Invitrogen), and all constructs were verified by DNA sequencing. Database searches used the SMART (http://smart.embl-heidelberg.de/) and Pfam (http://www.sanger.ac.uk/Software/Pfam/) databases. CD-Blast searches identify the UBX domain with an $E = 2 \times 10^{-5}$ and the N-terminal ubiquitin-like domain in the long form with $E = 0.046$.

Antisera and biochemistry

Antisera were raised in rabbits using a peptide corresponding to the TUG C terminus, CSLGKVPKWLKLPASKR, conjugated to KLH (Covance). TUG antisera were used at dilutions of 1:1,000–2,000 on western blots. Other antibodies used included those directed to the myc epitope (9E10, Roche), Flag epitope (M2, Sigma), V5 epitope (Invitrogen), GLUT4 C terminus (gift of M. Charron), GLUT1 (Chemicon), insulin receptor β-subunit (Transduction Labs) and transferrin receptor (Pharmingen and Santa Cruz Biotechnology). Phycoerythrin-conjugated secondary antibodies were from Jackson Immunoresearch. Human GLUT4 and GLUT1 clones tagged identically with the V5 epitope at their C terminus were from Invitrogen. 293T cells were transfected using Fugene 6 reagent (Roche). Immunoprecipitations were done in TNET or HNET (20 mM Tris pH 8.0 or 40 mM HEPES pH 7.5, with 150 mM NaCl, 2 mM EDTA, 1% Triton X-100) containing one Complete protease inhibitor tablet (Roche) per 20 ml, 20 mM iodoacetamide (Sigma), and (for 3T3-L1 cells) 50 mM octylglucoside (Roche) and 5 μg ml^{-1} MG-132 (Calbiochem). Cells were lysed for >30 min before pelleting of insoluble debris, and immunoprecipitations were allowed to proceed from 6 h to overnight at 4 °C. Immunoprecipitates were washed six times with the same buffer, and were eluted in SDS–PAGE (polyacrylamide gel electrophoresis) sample buffer for 10–15 min at 42 °C. Western blotting and subcellular fractionation were performed as described previously[3].

2-Deoxyglucose uptake

Assays were modified from ref. 21. 3T3-L1 adipocytes were seeded to 24-well plates, starved, washed with Krebs–Ringer phosphate buffer[21], and stimulated using 100 nM insulin for 20 min at 37 °C. 1 μCi ml^{-1} 2-deoxy-D-[2,6-^{3}H]glucose and 0.2 μCi ml^{-1} D-[1-^{14}C]mannitol were added so that the final concentration of 2-deoxyglucose was 50 μM. Uptake was at 37 °C for 6 min, then cells were washed with cold PBS and lysed in 300 μl per well TNET. [^{14}C]mannitol counts were used to control for residual extracellular 2-deoxyglucose, and nonspecific uptake was measured in the presence of 20 μM cytochalasin B. A portion of each lysate was used in a micro-BCA protein assay (Pierce), and counts were normalized to this measurement to control for variation in the number of cells in each well. Lysates were also immunoblotted to demonstrate equivalent expression of GLUT1 and GLUT4. Assays were done in quadruplicate. All cells contained the dual-tagged GLUT4 reporter, and control experiments showed that the presence of this protein did not contribute to glucose transport activity. Confidence intervals for the ratio of insulin-stimulated to basal deoxyglucose uptake were calculated using a *t*-test on log-transformed data.

Microscopy

3T3-L1 adipocytes expressing the GLUT4 reporter were reseeded to coverslips and used for microscopy as described previously[22]. Polyclonal anti-TUG antisera (1:250) and either monoclonal anti-myc (1:250) or anti-TfnR (5 μg per ml) antibodies were used with Alexa594-conjugated goat anti-rabbit IgG and Alexa488-conjugated goat anti-mouse or anti-rat IgG secondary antibodies (Molecular Probes). The myc epitope was stained to increase the signal over that due to GFP alone. Control images were acquired with each antibody individually and in the absence of primary antibody. Images were acquired on a Zeiss LSM 510 laser scanning confocal microscope.

Received 17 June; accepted 4 August 2003; doi:10.1038/nature01989.

1. Bryant, N. J., Govers, R. & James, D. E. Regulated transport of the glucose transporter GLUT4. *Nature Rev. Mol. Cell Biol.* **3,** 267–277 (2002).
2. Holman, G. D. & Sandoval, I. V. Moving the insulin-regulated glucose transporter GLUT4 into and out of storage. *Trends Cell Biol.* **11,** 173–179 (2001).
3. Bogan, J. S., McKee, A. E. & Lodish, H. F. Insulin-responsive compartments containing GLUT4 in 3T3-L1 and CHO cells: regulation by amino acid concentrations. *Mol. Cell. Biol.* **21,** 4785–4806 (2001).
4. Liu, X. *et al.* Generation of mammalian cells stably expressing multiple genes at predetermined levels. *Anal. Biochem.* **280,** 20–28 (2000).
5. Kondo, H. *et al.* p47 is a cofactor for p97-mediated membrane fusion. *Nature* **388,** 75–78 (1997).
6. Chu, K., Niu, X. & Williams, L. T. A Fas-associated protein factor, FAF1, potentiates Fas-mediated apoptosis. *Proc. Natl Acad. Sci. USA* **92,** 11894–11898 (1995).
7. Buchberger, A., Howard, M. J., Proctor, M. & Bycroft, M. The UBX domain: a widespread ubiquitin-like module. *J. Mol. Biol.* **307,** 17–24 (2001).
8. Yuan, X. *et al.* Solution structure and interaction surface of the C-terminal domain from p47: a major p97-cofactor involved in SNARE disassembly. *J. Mol. Biol.* **311,** 255–263 (2001).
9. Ladanyi, M. *et al.* The der(17)t(X;17)(p11;q25) of human alveolar soft part sarcoma fuses the TFE3 transcription factor gene to ASPL, a novel gene at 17q25. *Oncogene* **20,** 48–57 (2001).
10. Giorgino, F. *et al.* The sentrin-conjugating enzyme mUbc9 interacts with GLUT4 and GLUT1 glucose transporters and regulates transporter levels in skeletal muscle cells. *Proc. Natl Acad. Sci. USA* **97,** 1125–1130 (2000).
11. Becker, K., Schneider, P., Hofmann, K., Mattmann, C. & Tschopp, J. Interaction of Fas(Apo-1/CD95) with proteins implicated in the ubiquitination pathway. *FEBS Lett.* **412,** 102–106 (1997).
12. Wright, D. A., Futcher, B., Ghosh, P. & Geha, R. S. Association of human fas (CD95) with a ubiquitin-conjugating enzyme (UBC-FAP). *J. Biol. Chem.* **271,** 31037–31043 (1996).
13. Lalioti, V. S., Vergarajauregui, S., Pulido, D. & Sandoval, I. V. The insulin-sensitive glucose transporter, GLUT4, interacts physically with Daxx. Two proteins with capacity to bind Ubc9 and conjugated to SUMO-1. *J. Biol. Chem.* **277,** 19783–19791 (2002).
14. Shepherd, P. R. & Kahn, B. B. Glucose transporters and insulin action—implications for insulin resistance and diabetes mellitus. *N. Engl. J. Med.* **341,** 248–257 (1999).
15. Perera, H. K. I. Syntaxin 6 regulates Glut4 trafficking in 3T3-L1 adipocytes. *Mol. Biol. Cell* **14,** 2946–2958 (2003).
16. Katome, T. Use of RNA-interference-mediated gene silencing and adenoviral overexpression to elucidate the roles of AKT/protein kinase B isoforms in insulin actions. *J. Biol. Chem.* **278,** 28312–28323 (2003).
17. Inoue, M., Chang, L., Hwang, J., Chiang, S. H. & Saltiel, A. R. The exocyst complex is required for targeting of Glut4 to the plasma membrane by insulin. *Nature* **422,** 629–633 (2003).
18. Bose, A. *et al.* Glucose transporter recycling in response to insulin is facilitated by myosin Myo1c. *Nature* **420,** 821–824 (2002).
19. Wilson, V. G. & Rangasamy, D. Intracellular targeting of proteins by sumoylation. *Exp. Cell Res.* **271,** 57–65 (2001).
20. Naviaux, R. K., Costanzi, E., Haas, M. & Verma, I. M. The pCL vector system: rapid production of helper-free, high-titer, recombinant retroviruses. *J. Virol.* **70,** 5701–5705 (1996).
21. Tordjman, K. M., Leingang, K. A., James, D. E. & Mueckler, M. M. Differential regulation of two distinct glucose transporter species expressed in 3T3-L1 adipocytes: effect of chronic insulin and tolbutamide treatment. *Proc. Natl Acad. Sci. USA* **86,** 7761–7765 (1989).
22. Bogan, J. S. & Lodish, H. F. Two compartments for insulin-stimulated exocytosis in 3T3-L1 adipocytes defined by endogenous ACRP30 and GLUT4. *J. Cell Biol.* **146,** 609–620 (1999).

Supplementary Information accompanies the paper on **www.nature.com/nature**.

Acknowledgements We thank P. Bickel for help with cDNA library construction, G. Paradis for assistance with flow cytometry, J. Cresswell for technical assistance, and N.-W. Chi, J. Avruch, J. Dziura and K. Calia for advice and encouragement. We thank I. Verma for the pCL-Eco plasmid, G. Nolan for retroviral packaging cell lines, M. Charron for GLUT4 antisera, M. Krieger for CHO cells expressing the ecotropic murine retrovirus receptor, and N. Watson and S. Zarnegar for help with microscopy. This work used the W.M. Keck Foundation Biological Imaging Facility at the Whitehead Institute, and the Center for Cell Imaging at Yale University. This work was supported by a New Investigator Award from the Chestnut Hill Charitable Foundation to J.S.B., by a Career Development Award from the American Diabetes Association to J.S.B., by a Pilot and Feasibility Award from the NIH-sponsored Boston Area Diabetes Endocrinology Research Center to J.S.B., by a postdoctoral fellowship from the Ares-Serono Foundation to T.-S.T., and by NIH grants to H.F.L. and J.S.B.

Competing interests statement The authors declare that they have no competing financial interests.

Correspondence and requests for materials should be addressed to J.S.B. (jonathan.bogan@yale.edu). The cDNA sequences of the short and long TUG forms have been deposited in GenBank under accession numbers AY349132 and AY349133, respectfully.